RESEARCH ARTICLE

Quantitative Evaluation of Iron Content in Idiopathic Rapid Eye Movement Sleep Behavior Disorder

Junyan Sun, MD,[1] Zhaoyu Lai, MEng,[2*] Jinghong Ma, MD, PhD,[3] Linlin Gao, MD, PhD,[1] Meijie Chen, MD, PhD,[1] Jie Chen, MD, PhD,[1] Jiliang Fang, MD, PhD,[4] Yangyang Fan, MD,[4] Yan Bao, MD,[4] Dongling Zhang, MD,[1] Piu Chan, MD, PhD,[1,5,6,7] Qi Yang, MD, PhD,[8] Chenfei Ye, PhD,[2,9,10] Tao Wu, MD, PhD,[1,5,6,7] and Ting Ma, PhD[2,7,9,11]

[1]*Department of Neurobiology, Neurology and Geriatrics, Xuanwu Hospital of Capital Medical University, Beijing Institute of Geriatrics, Beijing, China*
[2]*School of Electronic and Information Engineering, Harbin Institute of Technology at Shenzhen, Shenzhen, Guangdong, China*
[3]*Department of Neurology, Xuanwu Hospital of Capital Medical University, Beijing, China*
[4]*Department of Radiology, Guang'anmen Hospital, China Academy of Chinese Medical Sciences, Beijing, China*
[5]*Clinical Center for Parkinson's Disease, Capital Medical University, Beijing, China*
[6]*Key Laboratory for Neurodegenerative Disease of the Ministry of Education, Beijing Key Laboratory for Parkinson's Disease, Parkinson Disease Center of Beijing Institute for Brain Disorders, Beijing, China*
[7]*National Clinical Research Center for Geriatric Disorders, Beijing, China*
[8]*Department of Radiology, Xuanwu Hospital of Capital Medical University, Beijing, China*
[9]*Peng Cheng Laboratory, Shenzhen, Guangdong, China*
[10]*Mindsgo Life Science Shenzhen Ltd, Shenzhen, Guangdong, China*
[11]*Advanced Innovation Center for Human Brain Protection, Capital Medical University, Beijing, China*

ABSTRACT: Background: Idiopathic rapid eye movement sleep behavior disorder is an early sign of neurodegenerative disease. This study aimed to quantitatively evaluate iron content in idiopathic rapid eye movement sleep behavior disorder patients using quantitative susceptibility mapping and to examine the potential of this technique to identify the prodromal stage of α-synucleinopathies.

Methods: Twenty-five idiopathic rapid eye movement sleep behavior disorder patients, 32 Parkinson's disease patients, and 50 healthy controls underwent quantitative susceptibility mapping. The mean magnetic susceptibility values within the bilateral substantia nigra, globus pallidus, red nucleus, head of the caudate nucleus, and putamen were calculated and compared among groups. The relationships between the values and the clinical features of idiopathic rapid eye movement sleep behavior disorder and Parkinson's disease were measured using correlation analysis.

Results: Idiopathic rapid eye movement sleep behavior disorder patients had elevated iron in the bilateral substantia nigra compared with healthy controls. Parkinson's disease patients had increased iron in the bilateral substantia nigra, globus pallidus, and left red nucleus compared with healthy controls and had elevated iron levels in the bilateral substantia nigra compared with idiopathic rapid eye movement sleep behavior disorder patients. Mean magnetic susceptibility values were positively correlated with disease duration in the left substantia nigra in idiopathic rapid eye movement sleep behavior disorder patients.

Conclusions: Quantitative susceptibility mapping can detect increased iron in the substantia nigra in idiopathic rapid eye movement sleep behavior disorder, which becomes more significant as the disorder progresses. This technique has the potential to be an early objective neuroimaging marker for detecting α-synucleinopathies.

Key Words: idiopathic rapid eye movement sleep behavior disorder (iRBD); iron content; Parkinson's disease (PD); quantitative susceptibility mapping (QSM)

***Correspondence to:** Tao Wu, MD, PhD, Department of Neurobiology, Neurology and Geriatrics, Xuanwu Hospital of Capital Medical University, Beijing Institute of Geriatrics, Beijing, China; wutao69@gmail.com; Ting Ma, PhD, School of Electronic and Information Engineering, Harbin Institute of Technology at Shenzhen, Shenzhen, Guangdong, China; tmahit@outlook.com.

Junyan Sun and Zhaoyu Lai contributed equally to the article.

Relevant conflicts of interest/financial disclosures: The authors have no conflicts of interest to report.

Funding agencies: This research was supported by the Ministry of Science and Technology (2016YFC1306503), the National Science Foundation of China (81571228), Beijing Municipal Commission of Health and Family Planning (Nos. PXM 2018_026283_000002), and the National Key Research and Development Program of China (2018YFC1312000).

Received: 25 July 2019; **Revised:** 7 October 2019; **Accepted:** 28 October 2019

Published online 00 Month 2019 in Wiley Online Library (wileyonlinelibrary.com). DOI: 10.1002/mds.27929

Idiopathic rapid eye movement sleep behavior disorder (iRBD) is characterized by the loss of muscular atonia and dream-enacting behaviors.[1,2] Longitudinal studies reported that 33.8% of clinically diagnosed iRBD patients developed neurodegenerative disorders within 4 years, especially α-synucleinopathies, such as Parkinson's disease (PD), dementia with Lewy bodies, and multiple system atrophy.[3-6] The conversion rate of iRBD to neurodegenerative disorders is 41% within 5 years[4] and 73.4% within 10 years.[6] Thus, iRBD is considered a prodromal stage of α-synucleinopathies.

It has been shown that abnormal metabolism of brain iron results in abnormal iron deposition in PD, which may contribute to the damage of dopaminergic neurons and the occurrence of typical clinicopathological lesions of PD. In addition, abnormal iron deposition can be detected using iron-sensitive magnetic resonance imaging (MRI).[7-10] It is thought that, as the prodromal stage of α-synucleinopathies, iRBD patients may also have increased iron deposition in the brain. A recent susceptibility weighted-imaging (SWI) study found loss of dorsolateral nigral hyperintensity in two-thirds of iRBD patients.[11] However, this study did not quantitatively analyze the iron content. Further, the judgment of absence of dorsolateral nigral hyperintensity is dependent on rater experience. In contrast, a couple of studies quantitatively evaluated iron content in iRBD using R2* mapping without finding a significant difference between iRBD patients and healthy controls (HCs).[12,13] It has been suggested that quantitative susceptibility mapping (QSM) is more sensitive, allowing for better detection of increased iron in PD compared with R2 and R2* mapping.[8,10,13,14] In addition, a postmortem validation study showed there was a strong correlation between iron content and magnetic susceptibility in gray matter.[15] Therefore, the purpose of this study was to employ QSM to quantitatively measure iron content in the gray matter of the brains in iRBD patients compared with PD patients. We hypothesized that iron deposition in iRBD patients would be higher than controls but lower than PD patients. This study will help to clarify the potential role of QSM as an imaging marker for prodromal α-synucleinopathies.

Materials and Methods

Participants

This experiment was performed in accordance with the Declaration of Helsinki and was approved by the Institutional Review Board of Xuanwu Hospital. All participants gave written informed consent prior to the experiment. All subjects (25 iRBD, 32 PD) were recruited from the Movement Disorders Clinic of the Xuanwu Hospital of Capital Medical University. PD patients were diagnosed according to the MDS Clinical Diagnostic Criteria.[16] The International Classification of Sleep Disorders-Third Edition (ICSD3) diagnostic criteria for RBD were used to screen patients for iRBD, which was later confirmed by polysomnography.[2] The inclusion criteria for 50 HCs were (1) older than 40 years, (2) no history of neurological or psychiatric

TABLE 1. Demographic and clinical data of participants and mean QSM values in each ROI

	HC (mean ± SD) n = 50	iRBD (mean ± SD) n = 25	PD(mean ± SD) n = 32	ANOVA *P*	*P* (post hoc)		
					HC vs iRBD	*iRBD* vs *PD*	*HC* vs *PD*
Sex (M/F)[a]	21/29	14/11	16/16	0.502	0.328	0.79	0.503
Age (years)	62.02 ± 7.52	62.48 ± 6.063	61.59 ± 6.52	0.891	1	1	1
RBDQ-HK	7.76 ± 5.382	41.84 ± 14.041	17.47 ± 13.198	< 0.001[c]	< 0.001[c]	< 0.001[c]	0.001[c]
UPDRS III	—	3.96 ± 3.565	23.66 ± 11.062	—	—	—	—
Duration(years)	—	4.16 ± 2.661	3.959 ± 3.42	—	—	—	—
H&Y	—	—	1.75 ± 0.67	—	—	—	—
SN-L(ppm)	0.089 ± 0.018	0.104 ± 0.016	0.121 ± 0.022	< 0.001[c]	0.003[c]	0.003[c]	< 0.001[c]
SN-R	0.09 ± 0.017	0.106 ± 0.015	0.12 ± 0.016	< 0.001[c]	< 0.001[c]	0.004[c]	< 0.001[c]
GP-L	0.096 ± 0.011	0.099 ± 0.019	0.111 ± 0.016	< 0.001[c]	1	0.014[b]	< 0.001[c]
GP-R	0.091 ± 0.013	0.099 ± 0.02	0.103 ± 0.013	0.002[c]	0.075	1	0.002[c]
RN-L	0.095 ± 0.014	0.104 ± 0.024	0.115 ± 0.024	<0.001[c]	0.305	0.09	< 0.001[c]
RN-R	0.094 ± 0.014	0.101 ± 0.022	0.106 ± 0.022	0.025[b]	0.523	0.872	0.022[b]
hCN-L	0.062 ± 0.01	0.066 ± 0.011	0.063 ± 0.01	0.205	0.227	0.868	1
hCN -R	0.059 ± 0.012	0.064 ± 0.011	0.06 ± 0.015	0.365	0.504	0.807	1
PU-L	0.063 ± 0.013	0.066 ± 0.012	0.063 ± 0.016	0.597	1	1	1
PU-R	0.062 ± 0.015	0.066 ± 0.011	0.057 ± 0.013	0.054	0.951	0.058	0.266

M, male; F, female; iRBD, idiopathic rapid eye movement sleep behavior disorder; PD, Parkinson's disease; HC, healthy control; RBDQ-HK, the REM Sleep Behavior Disorder Questionnaire–Hong Kong; UPDRS III, the Movement Disorder Society Unified Parkinson's Disease Rating Scale, part III; ppm, parts per million; SN, substantia nigra; GP, globus pallidus; RN, red nucleus; hCN, head of the caudate nucleus; PU, putamen; L, left; R, right; ANOVA, analyses of variance; —, not applicable.
[a]Pearson's chi-square test.
[b]$P < 0.05$.
[c]$P < 0.005$.

diseases, (3) no family history of movement disorders, and (4) no obvious cerebral lesions on MR structural images. The iRBD patients were evaluated using the Rapid Eye Movement Sleep Behavior Disorder Questionnaire–Hong Kong (RBDQ-HK) and the Movement Disorder Society Unified Parkinson's Disease Rating Scale, part III (MDS-UPDRS Ⅲ). PD patients were evaluated using the MDS-UPDRS Ⅲ scale while they were not taking any medication for PD. In addition, the Hoehn & Yahr (H&Y) scale was assessed in PD patients. Demographic details are summarized in Table 1.

MRI Data Acquisition

MRI data were acquired using a 3T scanner (MagnetomSkyra, Siemens, Germany) with a 20-channel receiver head and neck joint coil (16 channels open for scanning). PD patients were scanned after not taking their medication for a minimum of 12 hours. Whole-brain sagittal 3-dimensional (3-D) T1 magnetization-prepared rapid gradient-echo imaging was acquired with the following parameters: slice thickness, 1 mm; repetition time (TR), 2530 milliseconds; echo time (TE), 2.98 milliseconds; flip angle, 7°; display field of view (DFOV), 256 × 256 × 192 pixels; voxel size, 1 × 1 × 1 mm^3; scanning time, 5 minutes, 13 seconds. A 3-D single-echo gradient echo sequence was performed with the following parameters: slice thickness, 1.5 mm; TR, 25 milliseconds; TE, 17.5 milliseconds; echo number, 1; flip angle, 15°; DFOV, 256 × 256× 80 pixels; voxel size, 0.667 × 0.667 × 1.5 mm^3; scanning time, 5 minutes, 6 seconds.

Image Analysis

QSM Reconstruction

QSM reconstruction was performed using MATLAB-based susceptibility imaging software (STI Suite; https://people.eecs.berkeley.edu/~chunlei.liu/software.html).[17] The corrected and combined phase images were acquired by weighting the magnitude of the corresponding channel with the vendor-provided combination method[18] and were unwrapped using a Laplacian-phase unwrapping method.[17,19] Then, the phase-unwrapped images were used to remove the background field using the V-SHARP method.[20] To reduce extreme streaking artifacts caused

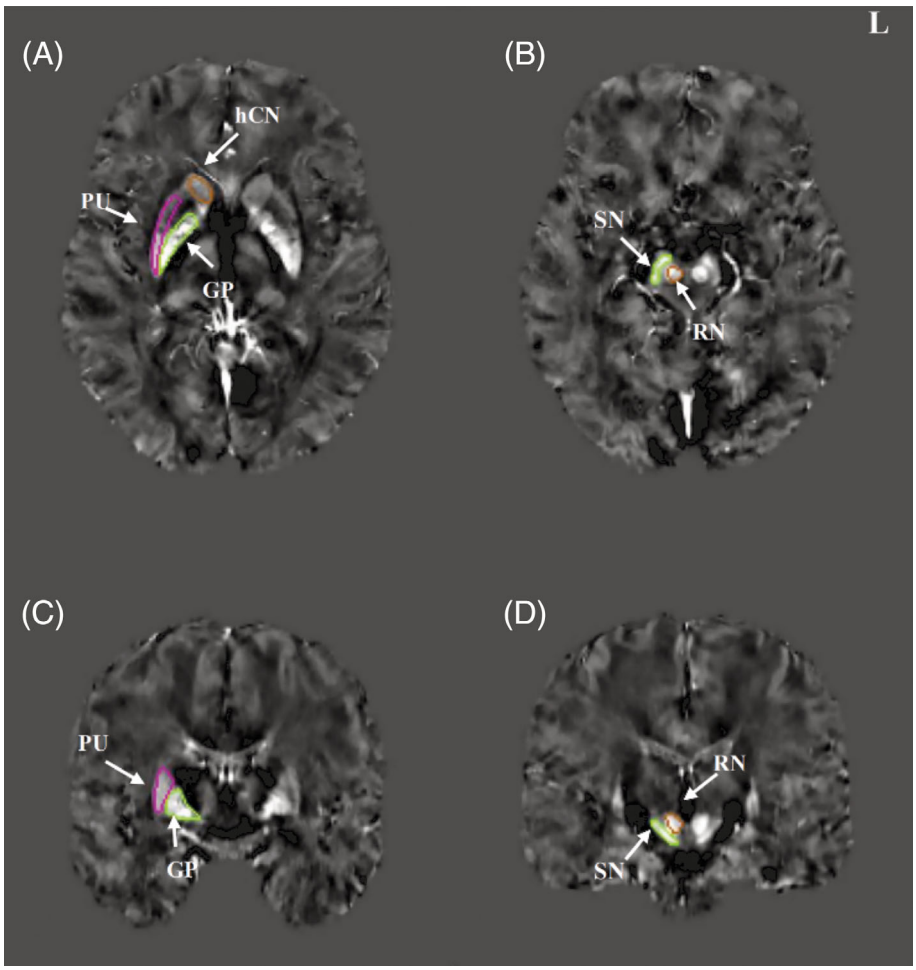

FIG. 1. The definition of regions of interest (ROIs). The ROIs included the substantia nigra (SN), globus pallidus (GP), red nucleus (RN), the head of the caudate nucleus (hCN), and putamen (PU) bilaterally.

by large veins, susceptibility maps were generated in the process of field-to-susceptibility inversion by using an improved sparse linear equation and least-squares algorithm (streaking artifact reduction for QSM, STAR-QSM).[21]

Image Processing

Image processing was performed using Advanced Normalization Tools (http://picsl.upenn.edu/software/ants/). The registration and normalization processes were completed as follows: (1) the magnitude and T1-weighted images were first skull-stripped using Brain Extraction Tools, and the QSM images were skull-stripped in the QSM reconstruction process (using STI Suite); (2) after the images had been skull-stripped, all magnitude images were coregistered to the individual T1-weighted images using a linear registration algorithm. Next, all the QSM images were brought directly to the individual T1-weighted space.[10]

Region-of-Interest Analysis

We selected 10 gray-matter brain areas as regions of interest (ROIs), including the substantia nigra (SN), globus pallidus (GP), red nucleus (RN), head of caudate nucleus (hCN), and putamen (PU) bilaterally (Fig. 1). The ROIs were manually plotted on each subject based on the anatomic structure of native space–reconstructed QSM images using DtiStudio and ROIEditor software (available at www.MriStudio.org). The SN was defined as the high-contrast region surrounded by tissue dorsal to the cerebral peduncle and ventral to the red nucleus.[22] We abided by the following principles when

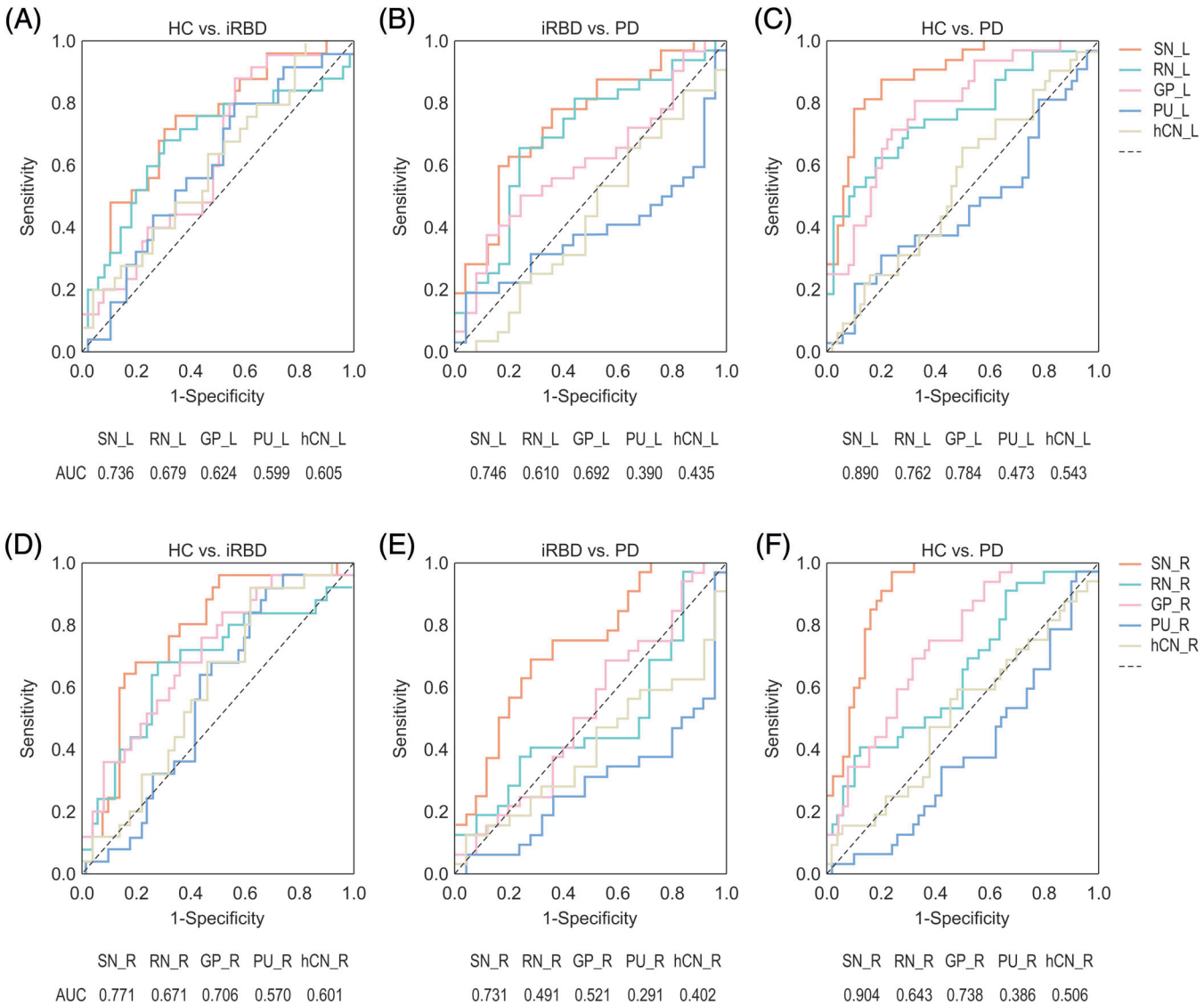

FIG. 2. Receiver operating characteristic (ROC) curves showing comparisons of the QSM values among the groups in each ROI. The diagnostic performance of the QSM values was defined by the area under the curve (AUC). [Color figure can be viewed at wileyonlinelibrary.com]

drawing the ROIs to avoid containing adjacent brain regions from separate ROIs: (1) draw all successive slices with a clear, visible boundary of the nucleus in the axial plane; (2) remove the first and last layers of the nucleus; (3) draw a pixel point inward to ensure that the region drawn is within the scope of the nucleus; and (4) avoid obvious vascular structures. The QSM values (referenced to the susceptibility in the bilateral posterior limb of the internal capsule, www.brainlabel.org)[23,24] were calculated. Mean QSM values within each ROI in each group are shown in Table 1. To assess the interrater reliability of segmenting ROIs, J.S. and D.Z. drew the ROIs independently. For the intrarater reliability assessment, J.S. drew the ROIs once and then drew them once again after 6 weeks.

Statistical Analyses

The normal distribution of data in each group was confirmed by the 1-sample Kolmogorov-Smirnov test. The Pearson chi-square test was applied for sex frequency among the groups. Analysis of variance (ANOVA) was performed to compare age and RBDQ-HK among the groups. The intraclass correlation efficient (ICC) was used to evaluate the intra- and interrater reliability of segmented ROIs. An ICC of 0.81 to 1.00 was considered excellent agreement, 0.61 to 0.80 good agreement, 0.41 to 0.60 moderate agreement, 0.21 to 0.40 for fair agreement, and 0.20 or less poor agreement.

Differences in the QSM values among the groups for each ROI were analyzed with ANOVA. Post hoc tests with a Bonferroni correction were used to control type I error rate inflation for intergroup comparisons, and a $P < 0.005$ was considered statistically significant at the global level. In addition, a $P < 0.05$ was used to find the ROIs that had between-group differences. The discriminative power of QSM values was evaluated with the receiver operating characteristic curve.

The relationship between QSM value and clinical assessment (RBDQ-HK, MDS-UPDRS Ⅲ, disease duration, and H&Y stage) in iRBD and PD patients was investigated using Pearson's correlation analysis ($P < 0.005$ was considered a significant correlation, and $P < 0.05$ was considered a correlation tendency). In addition, a correlation between QSM value and bilateral GP, hCN, and PU values was analyzed in the iRBD and PD patients. Statistical analyses were performed using IBM SPSS Statistics (version 25; IBM Corp., Armonk, NY).

Results

There were no statistically significant differences between groups regarding age and sex; however, there was a significant difference in RBDQ-HK score (Table 1). Interrater agreement was excellent for each ROI (all ICCs >0.9). Intrarater agreement was excellent for 9 ROIs, except for the left GP (ICC, 0.772), which achieved good agreement. The results of QSM analysis are shown in Table 1. There was a significant difference in QSM values among the groups in the bilateral SN, bilateral GP, and left RN ($P < 0.005$, ANOVA).

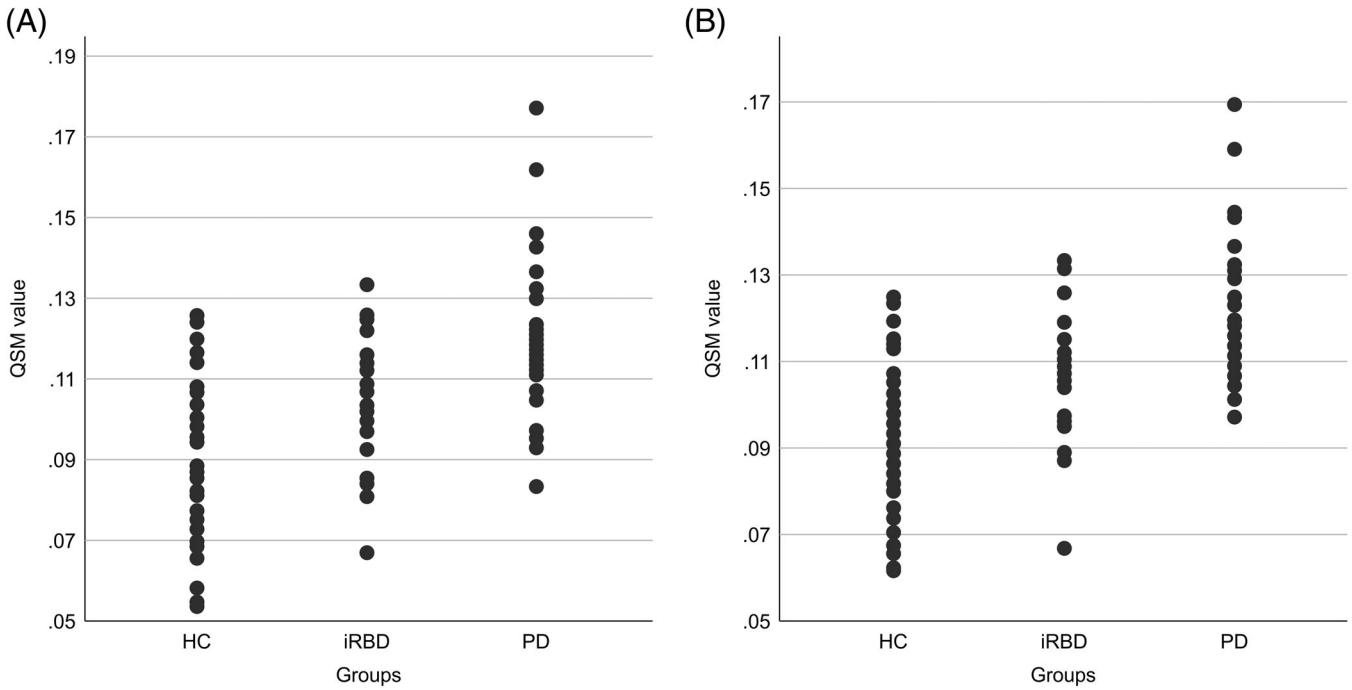

FIG. 3. The QSM values in the bilateral SN. (A) The QSM values in the left SN. (B) The QSM values in the right SN.

Patients with iRBD had significantly elevated iron content in the bilateral SN compared with the HCs ($P < 0.005$, post hoc test Bonferroni corrected). PD patients had significantly increased iron content in the bilateral SN, bilateral GP, and left RN compared to the HCs, and had significantly increased iron content in the bilateral SN compared with the iRBD patients ($P < 0.005$, post hoc test Bonferroni corrected). In addition, in PD patients, the QSM values in the right GP tended to be higher compared with the HCs, whereas the QSM values in the left GP tended to be higher compared with the iRBD patients ($P < 0.05$, post hoc test Bonferroni corrected).

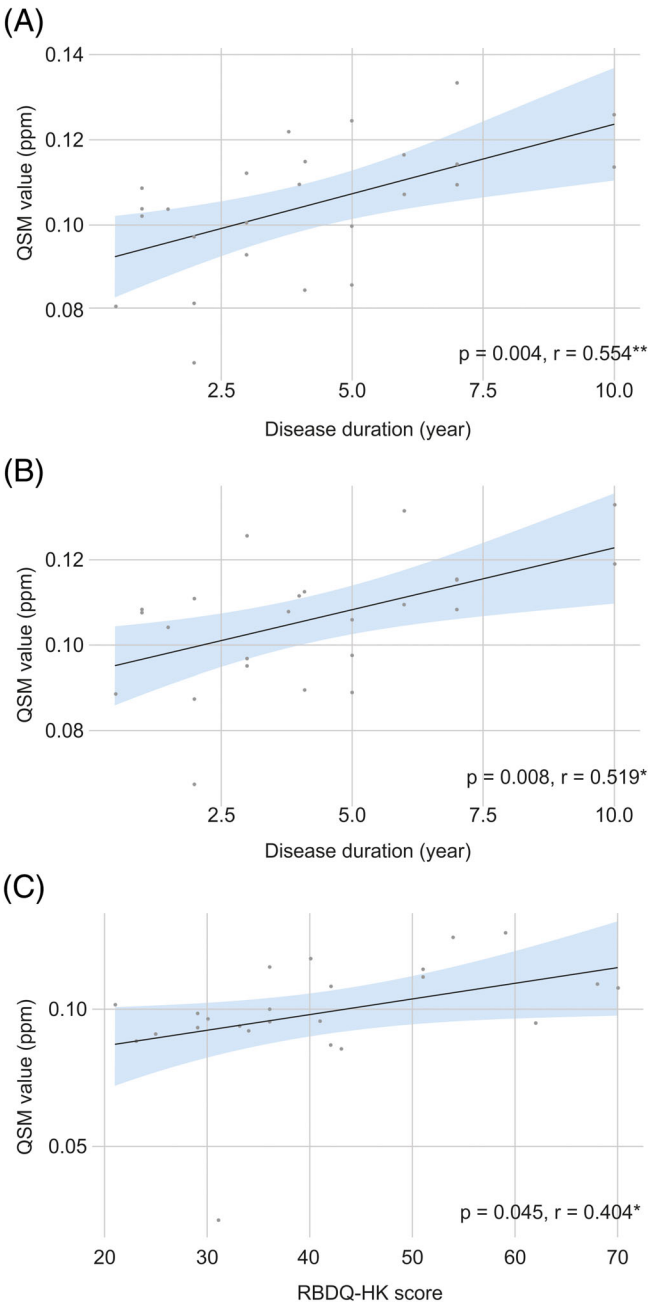

FIG. 4. Correlations between the QSM values and clinical features in iRBD patients. (A) Correlation between the QSM values and disease duration in the left SN. (B) Correlation between the QSM values and disease duration in the right SN. (C) Correlation between the QSM values and RBDQ-HK scores in the right GP. [Color figure can be viewed at wileyonlinelibrary.com]

The discriminative power of QSM values in each ROI is shown in Figure 2. We found that for the right SN, the accuracy of discrimination between PD patients and HCs was 0.904 (sensitivity, 0.969; specificity, 0.760); for iRBD patients versus HCs, accuracy, sensitivity, and specificity were 0.771, 0.680, and 0.800, respectively, whereas for iRBD versus PD patients, accuracy, sensitivity, and specificity were 0.731, 0.688, and 0.720, respectively. For the left SN, accuracy, sensitivity, and specificity were 0.890, 0.781, and 0.900, respectively, for PD patients versus HCs; 0.736, 0.760, and 0.660, repectively, for iRBD patients versus HCs; and 0.746, 0.594, and 0.840, respectively, for iRBD versus PD patients. The QSM values in the bilateral SN are shown in Figure 3.

In the iRBD patients, there was a significant positive correlation between QSM value and disease duration in the left SN ($r = 0.554$, $P = 0.004$; Fig. 4). In addition, QSM value tended to positively correlate with disease duration in the right SN ($r = 0.519$, $P = 0.008$; Fig. 4), as well as RBDQ-HK scores in the right GP ($r = 0.404$, $P = 0.045$; Fig. 4). In contrast, no significant correlation was found between QSM value and any of the clinical assessments (MDS-UPDRS Ⅲ, H&Y score, or disease duration) in the PD group. In addition, we did not find any significant correlation between iron content and volume of the striatum or pallidum in either the iRBD or PD groups.

Discussion

The main findings of the present study were that iron content is significantly elevated in the bilateral SN in iRBD patients compared with HCs and that there is a positive correlation between iron content and disease duration. In addition, PD patients had increased iron deposition in the bilateral SN, bilateral GP, and left RN compared with controls and a more prominent increase in iron content in the bilateral SN compared with iRBD patients.

The abnormal metabolism of iron has been suggested to induce an oxidative stress reaction and accelerate the aggregation of α-synuclein, which in turn contributes to the death of dopaminergic neurons in the SN, likely progressing to the basal ganglia and/or cerebral cortices.[25,26] Loss of the dopaminergic neurons in the SN is the pathological hallmark of PD. As approximately 40%–70% of dopaminergic neurons in the SN are lost at PD onset,[27] SN damage already exists before the onset of PD. Studies with various imaging modalities,

such as neuromelanin-sensitive MRI,[12] SWI,[11] diffusion tensor imaging,[12,28] and transcranial sonography,[3,28-30] have identified SN damage in iRBD patients. To the best of our knowledge, this is the first study that has quantitatively demonstrated increased iron content in the SN in iRBD patients. Previous studies using R2* mapping did not observe significantly increased iron content in the SN in iRBD patients compared with controls.[12,13] It has previously been shown that QSM is more sensitive, allowing for better detection of increased iron levels in PD patients, compared with R2* mapping.[8,10,13,14] Our findings demonstrate that QSM is able to quantitatively detect iron deposition in the prodromal stage of α-synucleinopathies.

Compared with PD patients, iRBD patients had significantly less iron content in the SN. In addition, QSM values tended to be higher in the left GP in PD patients compared with iRBD patients. This finding suggests that there may be a progressive increase in iron deposition in the SN and basal ganglia from the prodromal to the clinical stage of α-synucleinopathies, which is supported by our correlational analysis. We found that iron content in the left SN had a significant positive correlation with disease duration, whereas iron content in the right SN also tended to positively correlate with disease duration. These results indicate that iron deposition in the SN increases with the progression of iRBD. Although iron content in the GP did not significantly increase in iRBD patients, QSM value and RBDQ-HK score tended to positively correlate in the right GP, which indicates that iron deposition in the basal ganglia is related to the disease severity[31,32] of iRBD. As most iRBD patients develop α-synucleinopathies,[3-5,33] further longitudinal studies with QSM imaging are needed to investigate the relationship between gradually increased iron content in the SN and basal ganglia and the appearance of neurodegenerative symptoms. This will help better understanding of the progression from the prodromal stage to the clinical stage of α-synucleinopathies.

PD patients had significantly increased iron content in the bilateral SN, bilateral GP, and left RN compared with the HC group, which is consistent with previous reports.[10,34,35] Excessive iron likely contributes to the dysfunction of the nigrostriatal pathway,[35] which is heavily involved in the motor deficits seen in PD patients. We did not find a significant correlation between iron content and any of the clinical assessments in the PD group, which is inconsistent with some previous studies.[10,34,36] However, a recent study also did not find a correlation between iron content and clinical data in PD patients.[37] It is likely that we did not see a correlation in the present study, as most of our PD patients were in the early stages (average H&Y stage, 1.75 ± 0.67). Given the narrow spread of clinical results, the risk of false-negative associations is high. Future investigations regarding the relationship between QSM values and clinical data will require greater statistical power and more variance in the clinical data.

The QSM values in the bilateral SN showed high accuracy to discriminate PD patients from HCs (right SN, 0.904; left SN, 0.89) and moderate accuracy to discriminate iRBD patients from HCs (right SN, 0.771; left SN, 0.736), as well as to discriminate iRBD patients from PD patients (right SN, 0.731; left SN, 0.746). Our finding that QSM values in the SN can accurately discriminate PD patients and HCs is consistent with previous reports.[8,10] As iRBD is the prodromal stage of α-synucleinopathies, the QSM values of iRBD patients were between those of HCs and PD patients. Thus, it is not surprising that SN QSM values were less accurate in distinguishing between iRBD patients and HCs than they were for distinguishing between PD patients and HCs. The QSM values in the SN showed some overlap between iRBD patients and HCs (Fig. 3). Based on these findings, the QSM values of the whole SN can distinguish between iRBD patients and HCs at the group level; however, it is difficult to discriminate iRBD patients from HCs on an individual level. In the future, we plan to analyze QSM values in different subregions of the SN. We suspect that iron deposition in some subregions (eg, nigrosome 1) may be higher than in others and may show high accuracy in discriminating between iRBD patients and controls. In addition, the patients will be followed up to clarify whether iRBD patients with lower QSM values in the SN will not develop α-synucleinopathies or if the development of α-synucleinopathies will take longer than other iRBD patients.

There are some limitations to the current study. First, the sample size was relatively small; thus, larger cohorts are needed to validate the results. Second, because this was a cross-sectional study, we were unable to evaluate whether the iRBD patients developed α-synucleinopathies. To look at this, longitudinal studies are needed. Third, the nonisotropic resolution ($0.667 \times 0.667 \times 1.5$ mm^3) used in the current study can result in a loss of contrast in the QSM images, as well as errors in the estimation of the magnetic susceptibility values. However, with isotropic resolution, the scanning time is significantly prolonged compared with nonisotropic resolution. This is not ideal, as PD patients usually have difficulty staying inside the MRI scanner for long periods. In addition, long scanning periods may be accompanied by significant head movement in PD patients, thus resulting in worse image quality. Therefore, taking resolution and scan time into account, the application of nonisotropic resolution is accepted and has been applied in several studies on PD.[10,34,38]

In conclusion, using the QSM method, we demonstrated that iron content in iRBD patients is significantly increased in the SN and increases further as the disorder progresses. Our findings consequently suggest that the QSM technique has the potential to be an

objective neuroimaging marker for the detection of the prodromal stage of α-synucleinopathies.

Acknowledgments: This research was supported by the Ministry of Science and Technology (2016YFC1306503), the National Science Foundation of China (81571228), Beijing Municipal Commission of Health and Family Planning, No.PXM 2018_026283_000002, and the National Key Research and Development Program of China (2018YFC1312000).

References

1. Iranzo A, Santamaria J, Tolosa E. Idiopathic rapid eye movement sleep behaviour disorder: diagnosis, management, and the need for neuroprotective interventions. Lancet Neurol 2016;15(4):405–419.
2. American Academy of Sleep Medicine. International Classification of Sleep Disorders, 3rd ed. Darien, IL: American Academy of Sleep Medicine; 2014.
3. Iranzo A, Fernández-Arcos A, Tolosa E, et al. Neurodegenerative disorder risk in idiopathic REM sleep behavior disorder: study in 174 patients. PLoS One 2014;9(2):e89741.
4. Postuma RB, Iranzo A, Hogl B, et al. Risk factors for neurodegeneration in idiopathic rapid eye movement sleep behavior disorder: a multicenter study. Ann Neurol 2015;77(5):830–839.
5. Schenck CH, Boeve BF, Mahowald MW. Delayed emergence of a parkinsonian disorder or dementia in 81% of older men initially diagnosed with idiopathic rapid eye movement sleep behavior disorder: a 16-year update on a previously reported series. Sleep Med 2013;14(8):744–748.
6. Iranzo A, Tolosa E, Gelpi E, et al. Neurodegenerative disease status and post-mortem pathology in idiopathic rapid-eye-movement sleep behaviour disorder: an observational cohort study. Lancet Neurol 2013;12(5):443–453.
7. Martin-Bastida A, Politis M, Loane C, et al. Susceptibility Weighted Imaging to Detect Nigral Iron Accumulation in Parkinson's Disease. J Neurol Neurosurg Psychiatry 2015;86(11):e4.91–e94.
8. Barbosa JHO, Santos AC, Tumas V, et al. Quantifying brain iron deposition in patients with Parkinson's disease using quantitative susceptibility mapping, R2 and R2*. Magnetic Resonance Imaging 2015;33(5):559–565.
9. Graham JM, Paley MN, Grünewald RA, Hoggard N, Griffiths PD. Brain iron deposition in Parkinson's disease imaged using the PRIME magnetic resonance sequence. Brain 2000;123(Pt 12):2423–2431.
10. Du G, Liu T, Lewis MM, et al. Quantitative susceptibility mapping of the midbrain in Parkinson's disease. Mov Disord 2016;31(3):317–324.
11. De MR, Seppi K, Högl B, et al. Loss of Dorsolateral Nigral Hyperintensity on 3.0 Tesla Susceptibility-Weighted Imaging in Idiopathic Rapid Eye Movement Sleep Behavior Disorder. Ann Neurol 2016;79(6):1026–1030.
12. Pyatigorskaya N, Gaurav R, Arnaldi D, et al. Magnetic Resonance Imaging Biomarkers to Assess Substantia Nigra Damage in Idiopathic Rapid Eye Movement Sleep Behavior Disorder. Sleep 2017; 40(11) doi: https://doi.org/10.1093/sleep/zsx149.
13. Lee JH, Han YH, Cho JW, et al. Evaluation of brain iron content in idiopathic REM sleep behavior disorder using quantitative magnetic resonance imaging. Parkinsonism Relat Disord 2014;20(7):776–778.
14. Deistung A, Schafer A, Schweser F, Biedermann U, Turner R, Reichenbach JR. Toward in vivo histology: a comparison of quantitative susceptibility mapping (QSM) with magnitude-, phase-, and R2*-imaging at ultra-high magnetic field strength. Neuroimage 2013;65:299–314.
15. Langkammer C, Schweser F, Krebs N, et al. Quantitative susceptibility mapping (QSM) as a means to measure brain iron? A post mortem validation study. Neuroimage 2012;62(3):1593–1599.
16. Hughes AJ, Daniel SE, Kilford L, Lees AJ. Accuracy of clinical diagnosis of idiopathic Parkinson's disease: a clinico-pathological study of 100 cases. J Neurol Neurosurg Psychiatry 1992;55(3):181–184.
17. Wu B, Li W, Guidon A, Liu C. Whole brain susceptibility mapping using compressed sensing. Magn Reson Med 2012;67(1):137–147.
18. Prock T, Collins DJ, Dzik-Jurasz AS, Leach MO. An algorithm for the optimum combination of data from arbitrary magnetic resonance phased array probes. Phys Med Biol 2002;47(2):N39–N46.
19. Li W, Wu B, Liu C. Quantitative susceptibility mapping of human brain reflects spatial variation in tissue composition. Neuroimage 2011;55(4):1645–1656.
20. Wei L, Bing W, Anastasia B, et al. Differential developmental trajectories of magnetic susceptibility in human brain gray and white matter over the lifespan. Hum Brain Mapping 2014;35(6):2698–2713.
21. Wei H, Dibb R, Zhou Y, et al. Streaking artifact reduction for quantitative susceptibility mapping of sources with large dynamic range. NMR Biomed 2015;28(10):1294–1303.
22. Lehéricy S, Bardinet E, Poupon C, Vidailhet M, Francois C. 7 Tesla magnetic resonance imaging: a closer look at substantia nigra anatomy in Parkinson's disease. Mov Disord 2014;29(13):1574–1581.
23. Wu D, Ma T, Ceritoglu C, et al. Resource atlases for multi-atlas brain segmentations with multiple ontology levels based on T1-weighted MRI. Neuroimage 2016;125:120–130.
24. Straub S, Schneider TM, Emmerich J, et al. Suitable reference tissues for quantitative susceptibility mapping of the brain. Magn Reson Med 2017;78(1):204–214.
25. Apostolakis S, Kypraiou AM. Iron in neurodegenerative disorders: being in the wrong place at the wrong time? Rev Neurosci 2017;28 (8):893–911.
26. Ward RJ, Zucca FA, Duyn JH, Crichton RR, Zecca L. The role of iron in brain ageing and neurodegenerative disorders. Lancet Neurol 2014;13(10):1045–1060.
27. Bernheimer H, Birkmayer W, Hornykiewicz O, Jellinger K, Seitelberger F. Brain dopamine and the syndromes of Parkinson and Huntington Clinical, morphological and neurochemical correlations. J Neurol Sci 1973;20(4):415–455.
28. Unger MM, Möller JC, Stiasny-Kolster K, et al. Assessment of idiopathic rapid-eye-movement sleep behavior disorder by transcranial sonography, olfactory function test, and FP-CIT-SPECT. Mov Disord 2008;23(4):596–599.
29. Iranzo A, Lomeña F, Stockner H, et al. Decreased striatal dopamine transporter uptake and substantia nigra hyperechogenicity as risk markers of synucleinopathy in patients with idiopathic rapid-eye-movement sleep behaviour disorder: a prospective study [corrected]. Lancet Neurol 2010;9(11):1070–1077.
30. Iranzo A, Stockner H, Serradell M, et al. Five-year follow-up of substantia nigra echogenicity in idiopathic REM sleep behavior disorder. Mov Disord 2014;29(14):1774–1780.
31. Li SX, Wing YK, Lam SP, et al. Validation of a new REM sleep behavior disorder questionnaire (RBDQ-HK). Sleep Med 2010;11 (1):43–48.
32. Shen SS, Shen Y, Xiong KP, et al. Validation study of REM Sleep Behavior Disorder Questionnaire – Hong Kong (RBDQ-HK) in East China. Sleep Med 2014;15(8):952–958.
33. Iranzo A, Tolosa E, Gelpi E, et al. Neurodegenerative disease status and post-mortem pathology in idiopathic rapid-eye-movement sleep behaviour disorder: an observational cohort study. Lancet Neurol 2013;12(5):443–453.
34. He N, Ling H, Ding B, et al. Region-specific disturbed iron distribution in early idiopathic Parkinson's disease measured by quantitative susceptibility mapping. Hum Brain Mapp 2015;36(11):4407–4420.
35. Hare DJ, Double KL. Iron and dopamine: a toxic couple. Brain 2016;139(Pt 4):1026–1035.
36. Guan X, Xuan M, Gu Q, et al. Regionally progressive accumulation of iron in Parkinson's disease as measured by quantitative susceptibility mapping. NMR Biomed 2017;30(4) doi: https://doi.org/10.1002/nbm.3489.
37. Acosta-Cabronero J, Cardenas-Blanco A, Betts MJ, Butryn M, Nestor PJ. The whole-brain pattern of magnetic susceptibility perturbations in Parkinson's disease. Brain 2017;140(Pt 1):118–131.
38. Betts MJ, Acosta-Cabronero J, Cardenas-Blanco A, Nestor PJ, Duzel E. High-resolution characterisation of the aging brain using simultaneous quantitative susceptibility mapping (QSM) and R2* measurements at 7T. Neuroimage 2016;138:43–63.